ELECTRONIC SUPPLEMENTARY INFORMATION (ESI)

to

Hexanuclear $\{Zn^{II}_4Fe^{III}_2\}$ and $\{Zn^{II}_4Cr^{III}_2\}$ complexes from the use of potentially tetradentate NOO'O'' Schiff-base Ligands †

Konstantinos N. Pantelis [a], Sotiris G. Skiadas [a], Zoi G. Lada [b], Rodolphe Clérac [c], Yiannis Sanakis [*d], Pierre Dechambenoit [*c,] and Spyros P. Perlepes [*a,b]

[a] *Department of Chemistry, University of Patras, Patras 26504, Greece, E-mail: perlepes@upatras.gr*
[b] *Institute of Chemical Engineering Sciences (ICE-HT), Foundation for Research and Technology-Hellas (FORTH), Platani, P.O. Box 144, Patras 26504, Greece*
[c] *Univ. Bordeaux, CNRS, CRPP, UMR 5031, F-33600 Pessac, France, E-mail: pierre.dechambenoit@u-bordeaux.fr*
[d] *Institute of Nanoscience and Nanotechnology, NCSR "Demokritos", Aghia Paraskevi Attikis 15310, Greece, Email: i.sanakis@inn.demokritos.gr*

†Dedicated to Professor Mark Turnbull on the occasion of his retirement; a great inorganic chemist and magnetochemist, a precious friend.

Table S1 Crystallographic data for complexes $[Zn_4Fe_2(saphCOO)_6(NO_3)_2(EtOH)_2]\cdot 4CH_2Cl_2\cdot 2EtOH$ (**1**$\cdot 4CH_2Cl_2\cdot 2EtOH$), $[Zn_4Cr_2(saphCOO)_6(NO_3)_2(H_2O)_2]\cdot 4MeCN\cdot 2EtOH$ (**2**$\cdot 4MeCN\cdot 2EtOH$) and $[Zn_4Fe_2(4ClsaphCOO)_6(NO_3)_2(EtOH)_2]\cdot 4CH_2Cl_2\cdot 2EtOH$ (**3**$\cdot 4CH_2Cl_2\cdot 2EtOH$)

Compound	**1**$\cdot 4CH_2Cl_2\cdot 2EtOH$	**3**$\cdot 4CH_2Cl_2\cdot 2EtOH$	**2**$\cdot 4MeCN\cdot 2EtOH$
Formula	$C_{88}H_{66}Fe_2N_8O_{26}Zn_4\cdot 4(CH_2Cl_2), \cdot 2(C_2H_6O)$	$C_{88}H_{60}Cl_6\ Fe_2N_8O_{26}Zn_4\cdot 4(CH_2Cl_2)\cdot 2(C_2H_6O)$	$C_{84}H_{58}Cr_2N_8O_{26}Zn_4\cdot, 2(C_2H_6O)\cdot 4(C_2H_3N)$
FW (g·mol^{-1})	2456.50	2663.16	2217.21
Crystal color	brown	brown	red
Crystal size (mm)	0.24 x 0.17 x 0.10	0.09 x 0.07 x 0.02	0.11 x 0.05 x 0.03
Crystal system	monoclinic	triclinic	triclinic
Space group	$P2_1/c$	P-1	P-1
Temperature	120 K	120 K	120 K
***a* (Å)**	12.175(3)	12.2993(11)	12.3043(5)
***b* (Å)**	27.856(7)	15.6707(13)	14.2093(6)
***c* (Å)**	16.416(3)	15.6934(13)	15.7458(7)
***α* (°)**	90	67.497(3)	109.169(2)
***β* (°)**	113.189(15)	72.688(3)	90.594(2)
***γ* (°)**	90	83.591(3)	113.395(2)
***V* (Å^3)**	5118(2)	2667.8(4)	2354.85(18)
Z	2	1	1
d_{calc}	1.594	1.658	1.563
μ (mm^{-1})	1.488	1.579	1.312
θ_{min} - θ_{max}	1.462 ° - 23.565°	1.734° - 21.529°	1.828° - 25.091°
Refl. coll. / unique	61656 / 7381	55061 / 6132	87772 / 8353
Completeness to 2θ	0.967	0.996	0.997
R_{int}	0.1004	0.0938	0.1684
Refined param./restr.	660 / 12	681 / 18	650 / 2
$^aR_1$ ($I > 2\sigma(I)$)	0.0791	0.0423	0.0326
$^bwR_2$ (all data)	0.2076	0.1099	0.0866
Goodness of fit	1.181	1.056	1.009
CCDC number	2316071	2316072	2316073

^{a} $R_1 = \Sigma(|F_o|-|F_c|)/\Sigma(|F_o|)$

^{b} $wR_2 = \{\Sigma[w(F_o^2-F_c^2)^2]/\Sigma[w(F_o^2)^2]\}^{1/2}$

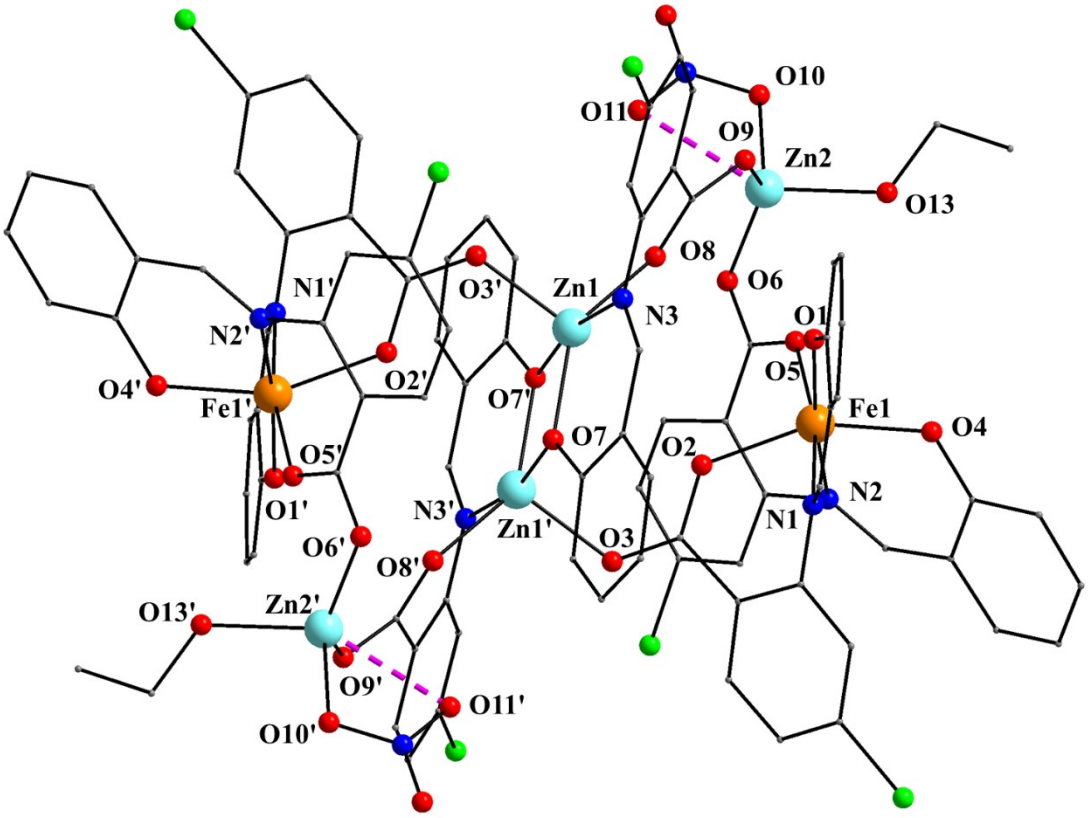

Fig. S1 Partially labeled plot of the molecule $[Zn_4Fe_2(4ClsaphCOO)_6(NO_3)_2(EtOH)_2]$ that is present in the crystal structure of **3**·$4CH_2Cl_2$·2EtOH. The dashed lines indicate a weakly bonding interaction, i.e. semicoordination. Symmetry operation used to generate equivalent atoms: (') – *x* + 1, - *y* + 1, - *z* + 2.

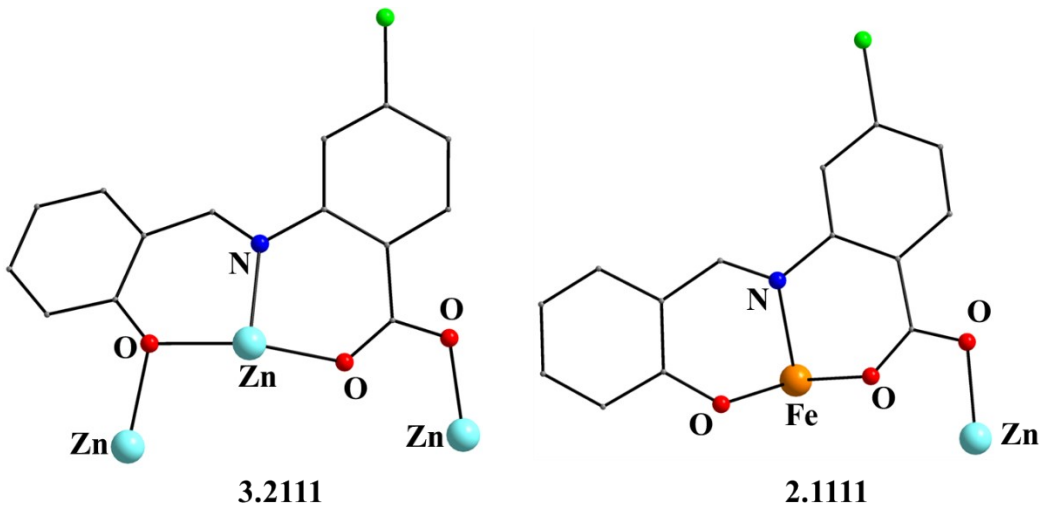

Fig. S2 The coordination modes (using Harris notation) of the $4ClsaphCOO^{2-}$ ligands in complex **3**·$4CH_2Cl_2$·2EtOH; four ligands adopt the 2.1111 ligation mode and two the 3.2111 one.

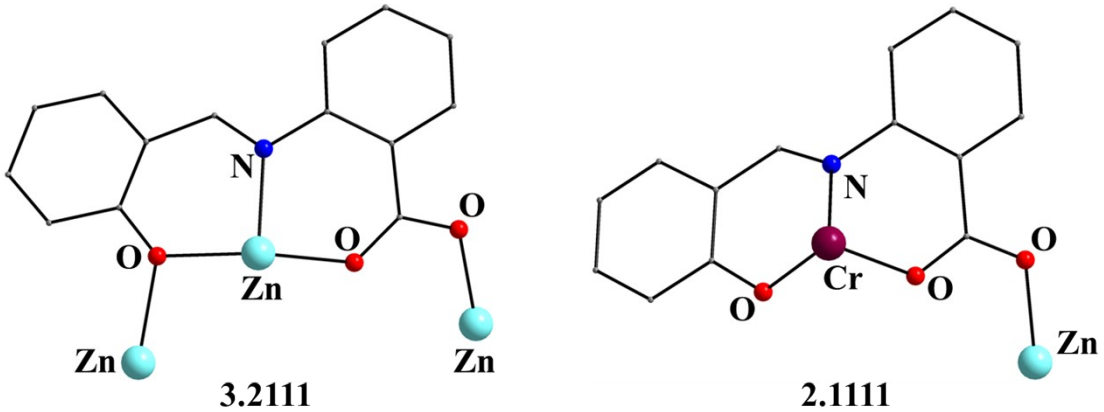

Fig. S3 The coordination modes (using Harris notation) of the saphCOO^{2-} ligands in complex **2**·4MeCN·2EtOH; four ligands adopt the 2.1111 ligation mode and two the 3.2111 one.

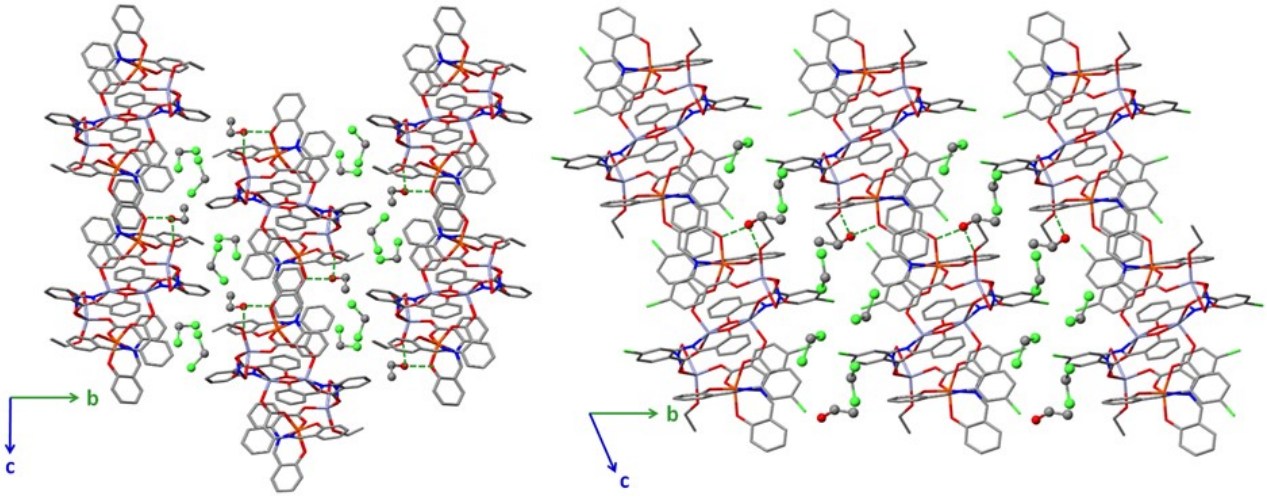

Fig. S4 Stick representations of **1**·4CH_2Cl_2·2EtOH (left) and **3**·4CH_2Cl_2·2EtOH (right) in the (bc) plane, showing the packing of the complexes separated by lattice CH_2Cl_2 molecules (depicted in ball and stick representation). H atoms are omitted for clarity. Intermolecular H bonds are illustrated with dashed green lines. C, grey; H, white; N, blue; O, red; Cl, light green; Fe, orange; Zn, light blue.

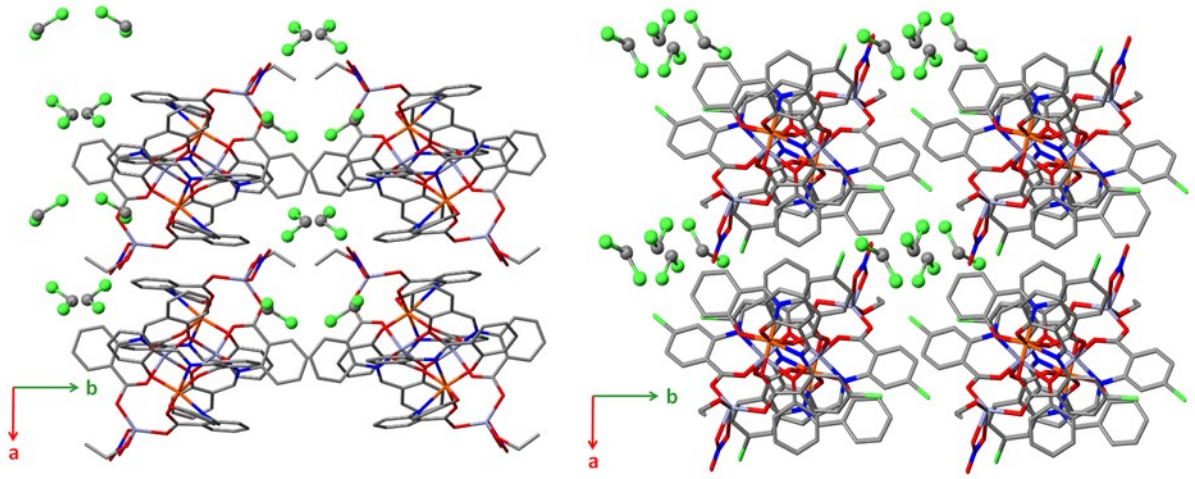

Fig. S5 Stick representations of **1**·4CH_2Cl_2·2EtOH (left) and **3**·4CH_2Cl_2·2EtOH (right) in the (ab) plane, showing the packing of the complexes separated by lattice CH_2Cl_2 molecules (depicted in ball and stick representation). H atoms and lattice EtOH molecules are omitted for clarity. Intermolecular H bonds are illustrated with dashed green lines. C, grey; H, white; N, blue; O, red; Cl, light green; Fe, orange; Zn, light blue.

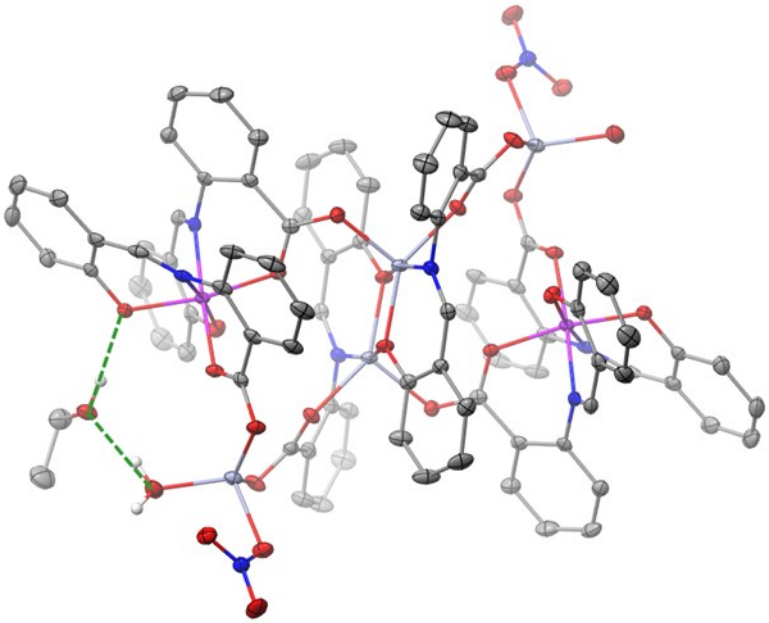

Fig. S6 ORTEP-type view of complex **2**·4MeCN·2EtOH and the H-bonded EtOH molecules in the crystal at 120 K. Thermal ellipsoids are depicted at a 50% probability level. Lattice MeCN molecules and H atoms are omitted for clarity, except those involved in H-bonding. H bonds are depicted in dashed green lines. C, grey; H, white; N, blue; O, red; Cr, purple; Zn, light blue.

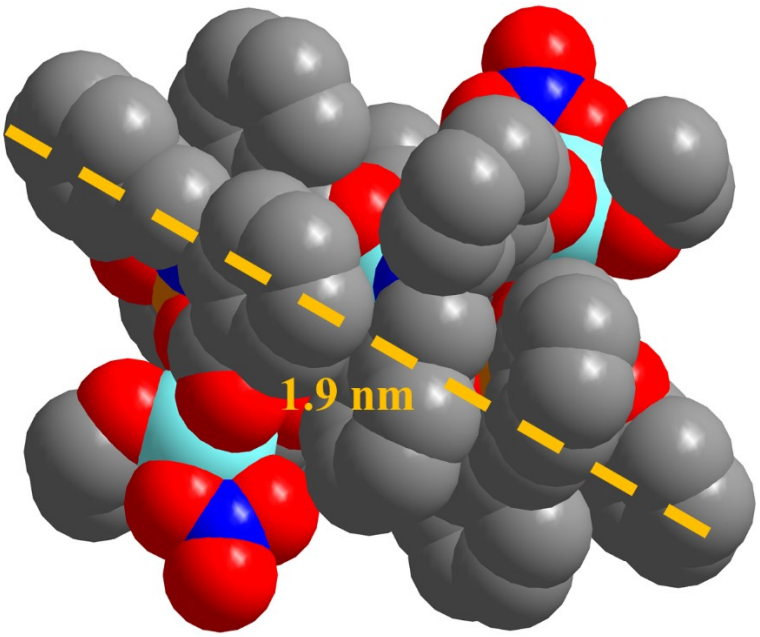

Fig. S7 Space-filling diagram of **1**.

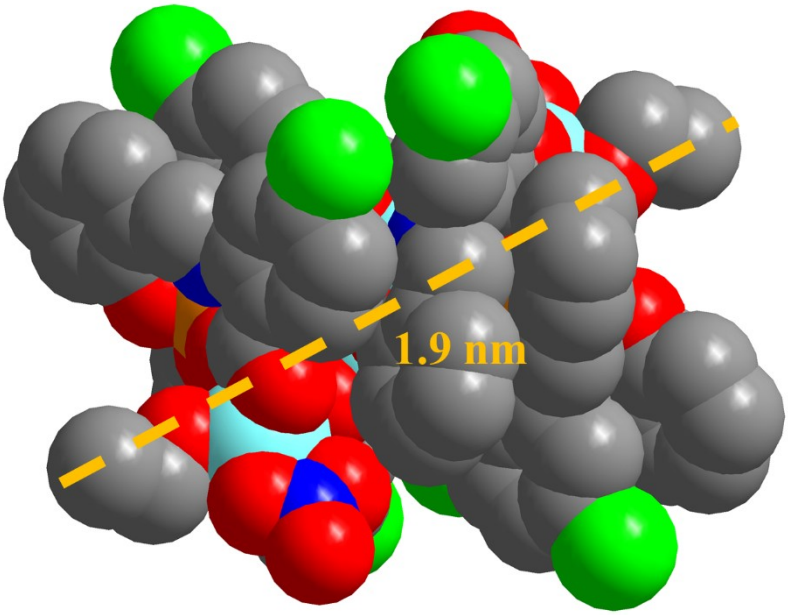

Fig. S8 Space-filling diagram of **3**.

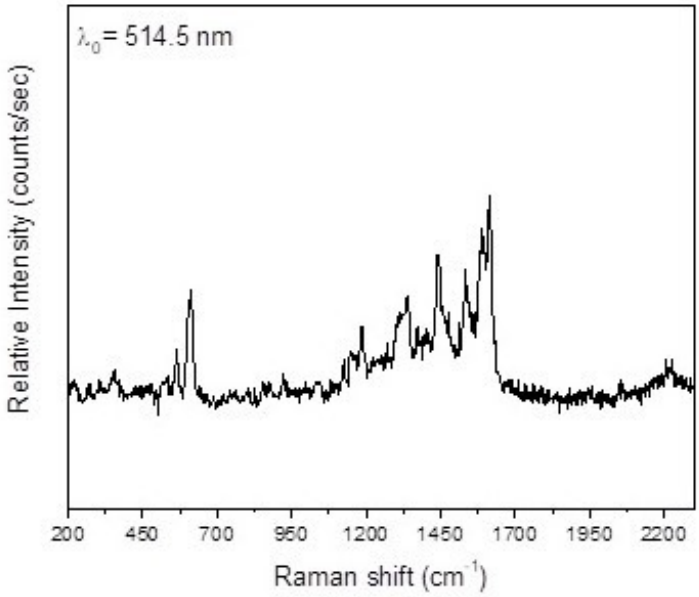

Fig. S9 The Raman spectrum of a dried sample of **1** in the 2300-200 cm^{-1} region.

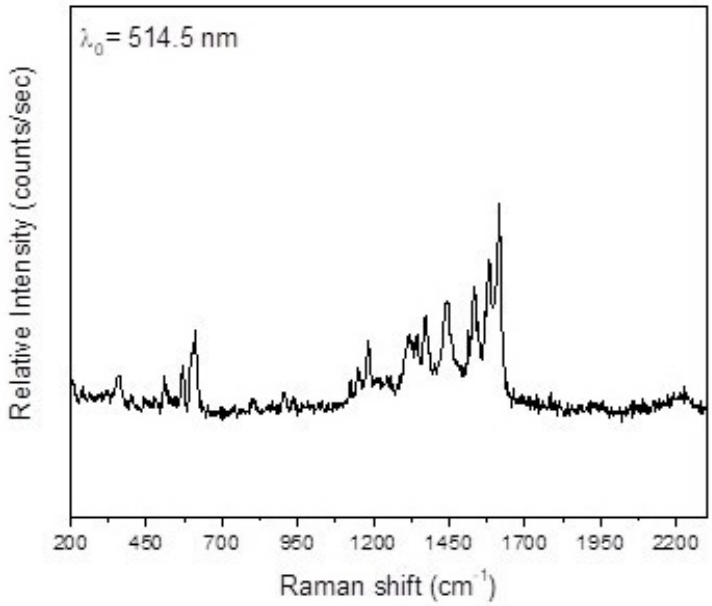

Fig. S10 The Raman spectrum of a dried sample of **3** in the 2300-200 cm^{-1} region.

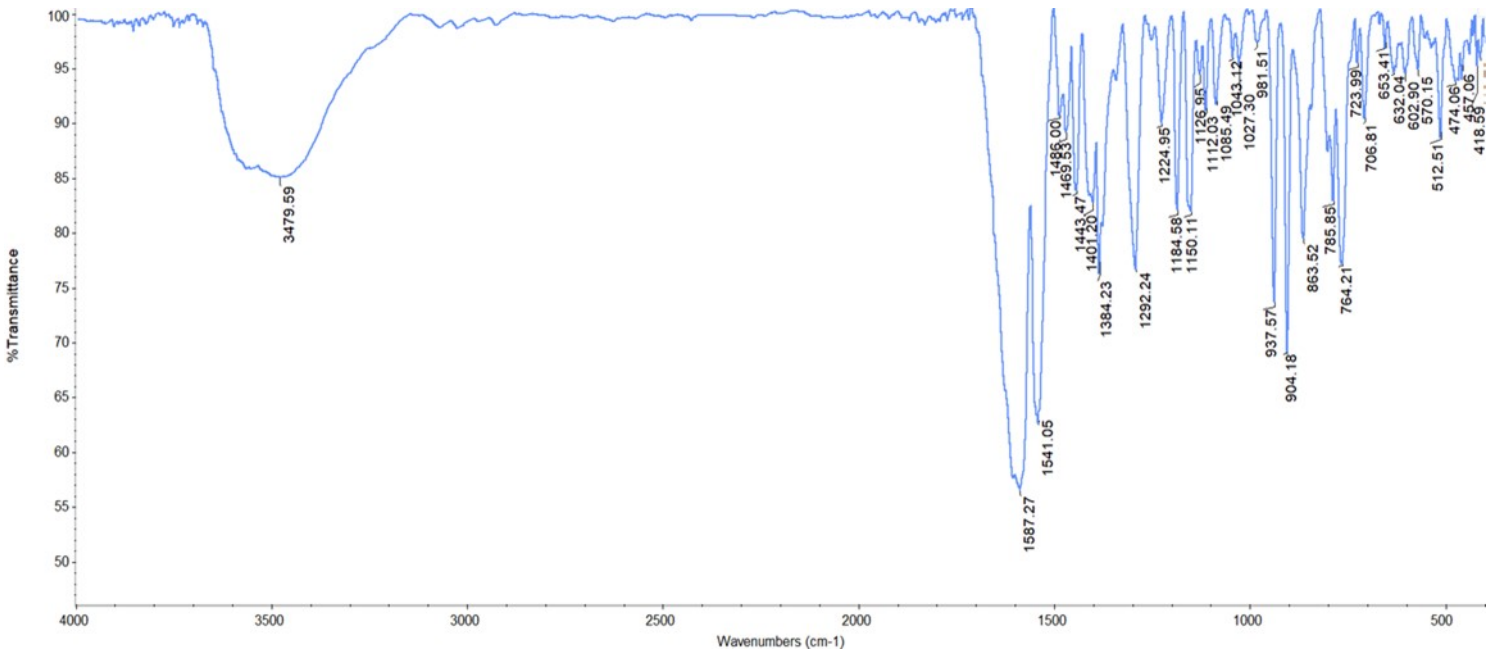

Fig. S11 The IR spectrum (KBr, cm^{-1}) of a dried sample of **3**.

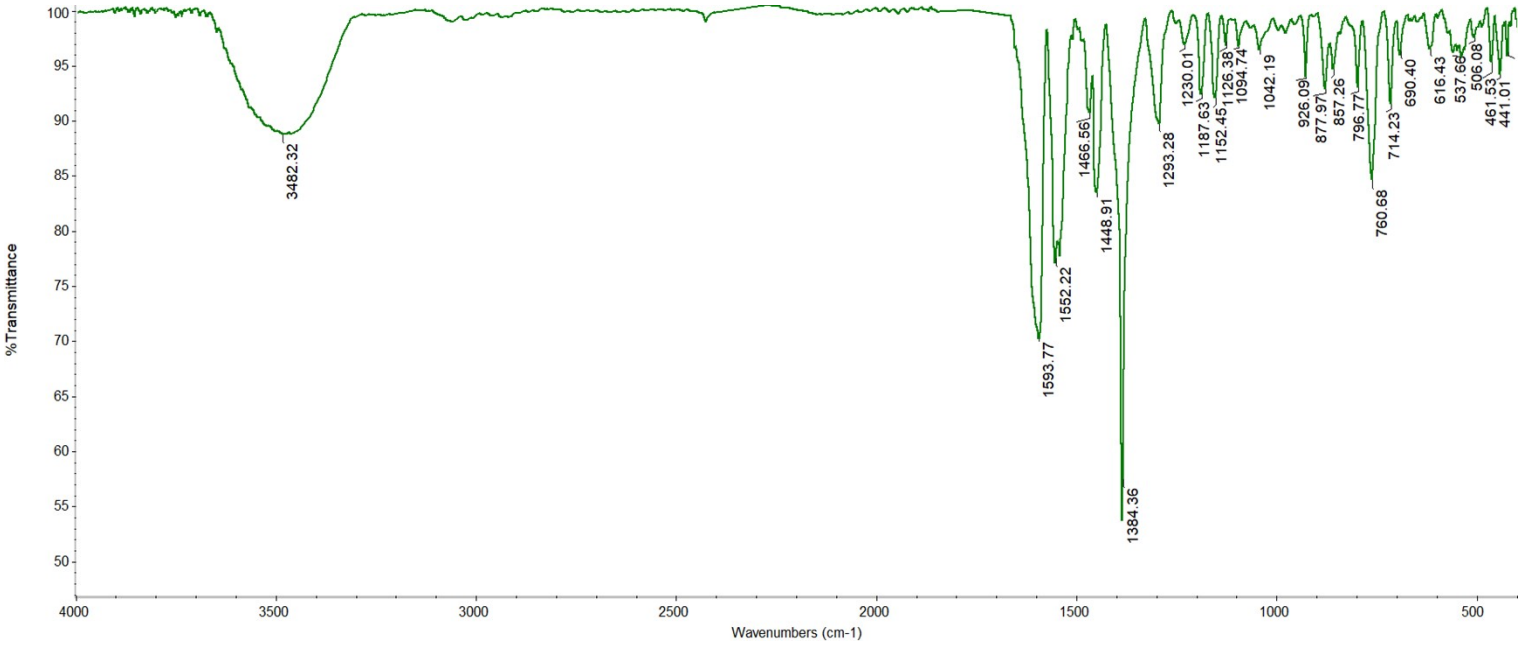

Fig. S12 The IR spectrum (KBr, cm^{-1}) of a dried sample of **2**.

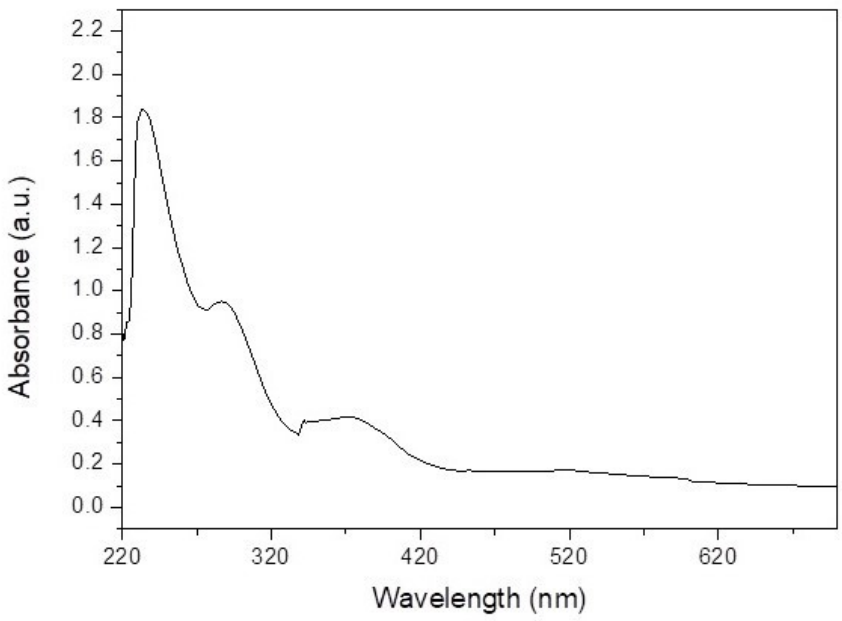

Fig. S13 The UV/Vis spectrum of a dried sample of **3** in CH_2Cl_2. The 340 nm peak is a ghost peak due to the instrument used.

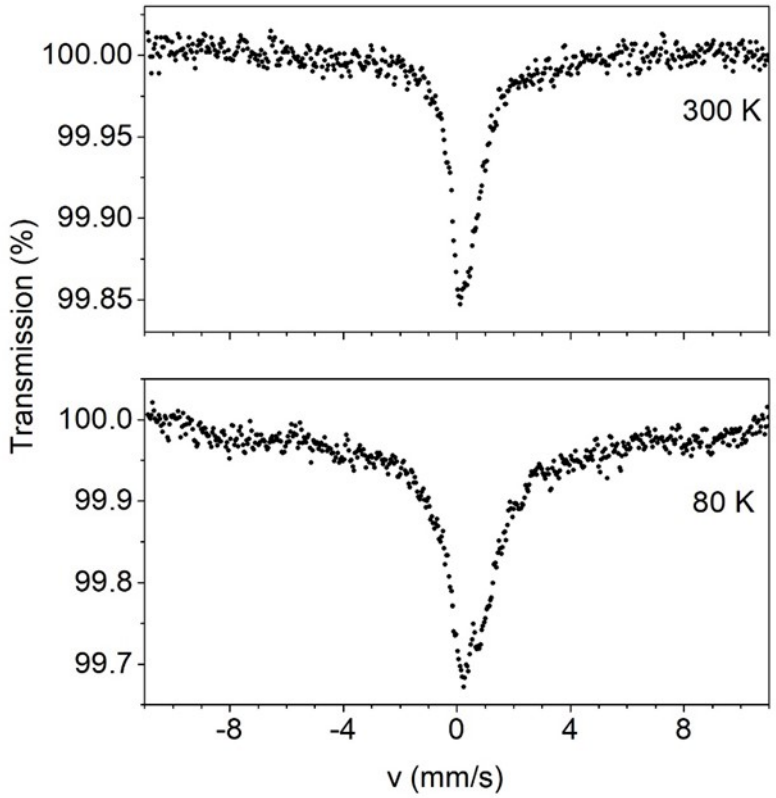

Fig. S14 Mössbauer spectra of powdered samples of complex **1** recorded at 300 and 80 K in zero applied field.

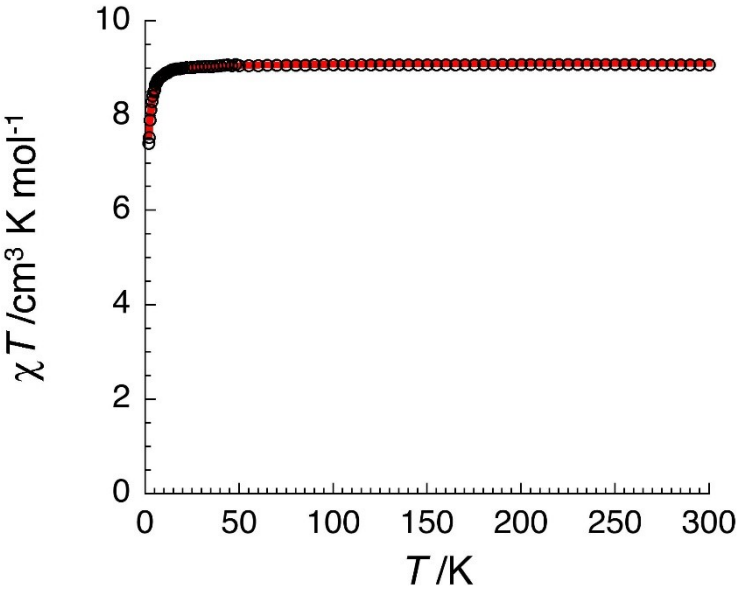

Fig. S15 Temperature dependence of the χT product (where χ is the molar magnetic susceptibility that equals M/H per complex, and T the temperature) collected in an applied dc magnetic field (H) of 0.1 T for **3**·4CH_2Cl_2·2EtOH. The solid red line is the best fit of the experimental data to an Heisenberg S_{Fe} = 5/2 spin dimer model as discussed in the text (with $\boldsymbol{H} = -2J(S_{Fe1} \bullet S_{Fe2})$: J/k_B = -0.06(1) K and g = 2.04(5)).

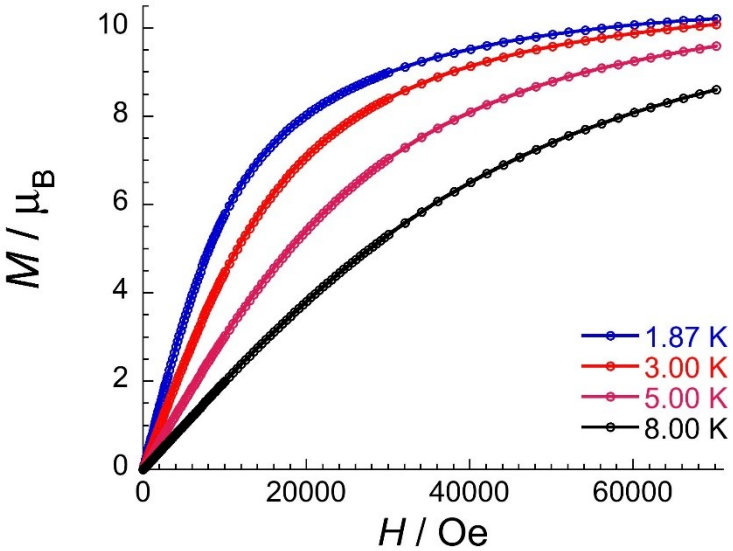

Fig. S16 Field dependence of the magnetization (M) for **3**·4CH_2Cl_2·2EtOH below 8 K (M(1.87 K, 7 T) = 10.2 μ_B implying g = 2.04).

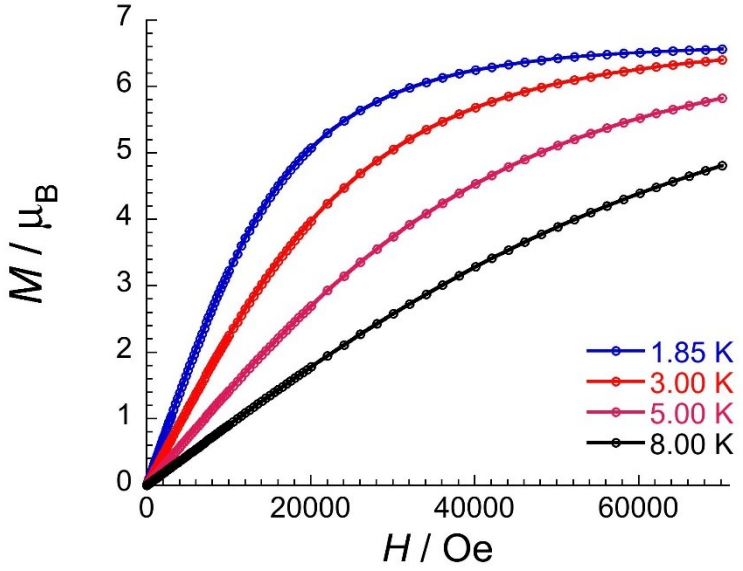

Fig. S17 Field dependence of the magnetization (*M*) for **2**·4MeCN.2EtOH below 8 K (*M*(1.85 K, 7 T) = 6.6 μ_B implying *g* = 2.20).

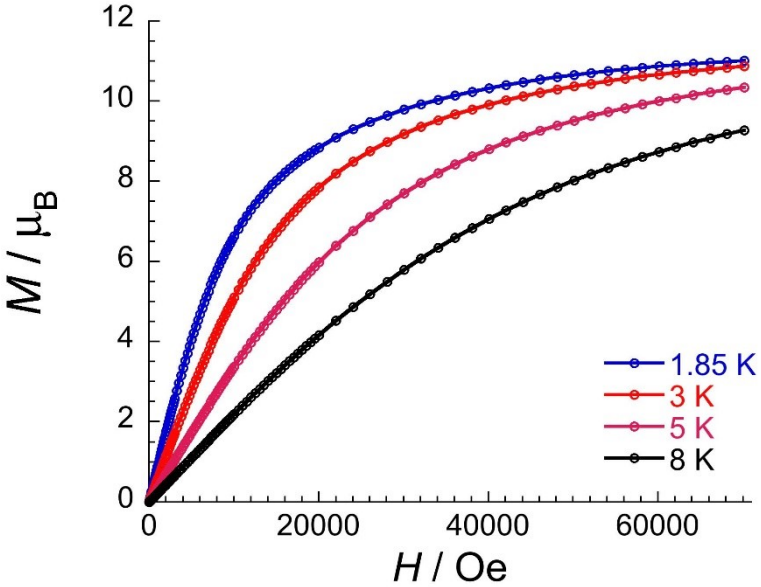

Figure S18 Field dependence of the magnetization (*M*) for **1**·4CH_2Cl_2·2EtOH below 8 K (*M*(1.85 K, 7 T) = 11.0 μ_B implying *g* = 2.10).